

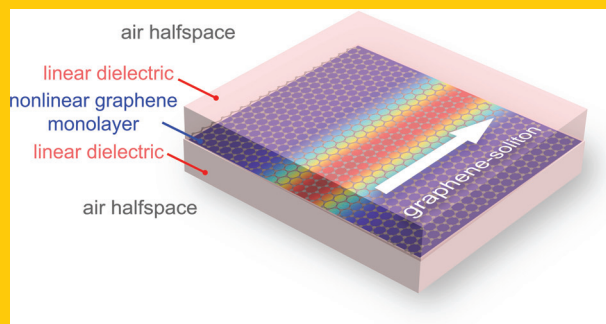
www.lpr-journal.org

LASER & PHOTONICS REVIEWS

WILEY-VCH

REPRINT

Abstract Nonlinear propagation of light in a graphene monolayer is studied theoretically. It is shown how the large intrinsic nonlinearity of graphene at optical frequencies enables the formation of quasi one-dimensional self-guided beams (spatial solitons) featuring subwavelength widths at moderate electric-field peak intensities. A novel class of nonlinear self-confined modes resulting from the hybridization of surface plasmon polaritons with graphene optical solitons is also demonstrated.

LETTER
ARTICLE

Graphene supports the propagation of subwavelength optical solitons

Maxim L. Nesterov¹, Jorge Bravo-Abad¹, Alexey Yu. Nikitin², Francisco J. García-Vidal^{1,3,*}, and Luis Martin-Moreno²

The experimental discovery and isolation of graphene monolayers from bulk graphite [1] has attracted great interest during the last years. The study of graphene properties has become a hot topic of research within the physics and nanoscience communities [2] as it promises, among others, a variety of optical and opto-electronical applications [3,4]. Very large values of the nonlinear optical susceptibilities corresponding to multiple harmonic generation were theoretically predicted [5,6] and have been experimentally verified very recently in the case of third-order nonlinear effects [7]. Still, it is an open question whether this high nonlinear coefficient, which occurs in a two-dimensional (2D) system, could induce strong nonlinear effects in electromagnetic (EM) modes that extend on the three spatial dimensions.

One of the nonlinear effects with greater potential for controlling light propagation at the micro- and nano-scales is the formation of temporal and spatial EM solitons [8–12]. In this Letter we demonstrate that 2D graphene monolayers support spatial non-diffracted beams (i.e., solitons) of subwavelength width in the optical regime. We illustrate this capability by analyzing two arrangements leading to solitons with different polarizations: a graphene monolayer embedded into a conventional dielectric waveguide and a graphene sheet placed on top of a metal-dielectric structure. We analyze in detail the formation of spatial solitons and the relation between soliton width and input intensity, showing that the subwavelength scale can be reached by

using feasible values for the beam peak intensity. We also develop a quasi-analytical model that is able to capture the basic ingredients of the numerical results.

The first structure in our analysis consists of a single graphene monolayer placed inside a planar linear dielectric waveguide, see Fig. 1 (a). This dielectric waveguide provides vertical confinement in the x -direction for the propagating EM mode. Graphene must be *physically* considered as a 2D material with nonlinear conductivity. But *mathematically* we can also approximate graphene by a very thin layer of a finite thickness introducing an *effective dielectric constant*. Then we can treat graphene using the Maxwell equations for bulk media. We have checked that both 2D and 3D approaches give virtually the same numerical results. Thus, we take directly the nonlinear susceptibility from the experiment, and approximate graphene by a thin $d_{\text{gr}} = 0.3$ nm-thick layer. The nonlinear polarization density in graphene is $\mathbf{P}_{\text{NL}}(\mathbf{r}, t) = \epsilon_0 \epsilon_{\text{NL}}(\mathbf{r}, t) \mathbf{E}_{\parallel}(\mathbf{r}, t)$, where $\mathbf{E}_{\parallel}(\mathbf{r}, t)$ is the in-plane component of the electric field (in y, z -plane) and $\epsilon_{\text{NL}}(\mathbf{r}, t) = \chi_{\text{gr}}^{(3)} [\mathbf{E}_{\parallel}(\mathbf{r}, t)]^2$ is the nonlinear contribution to the equivalent permittivity of the graphene layer. From the polarization density the nonlinear current is obtained as $\mathbf{j}_{\text{NL}}(\mathbf{r}, t) = \partial \mathbf{P}_{\text{NL}}(\mathbf{r}, t) / \partial t$. Throughout this paper, we consider the operating wavelength, $\lambda_0 = 850$ nm, for which a Kerr-type third-order effective nonlinear susceptibility $\chi_{\text{gr}}^{(3)} \simeq 1.5 \times 10^{-7}$ esu, ($\chi_{\text{gr}}^{(3)} \simeq 2.095 \times 10^{-15}$ m²/V² in SI units) has been measured [7]. The nonlinear eigenmode problem is formulated in terms of the 3D

¹ Departamento de Física Teórica de la Materia Condensada, Universidad Autónoma de Madrid, E-28049, Madrid, Spain

² Instituto de Ciencia de Materiales de Aragón and Departamento de Física de la Materia Condensada, CSIC-Universidad de Zaragoza, E-50009 Zaragoza, Spain

³ CIC nanoGUNE Consolider, E-20018 Donostia/San Sebastian, Spain

*Corresponding author(s): e-mail: fj.garcia@uam.es

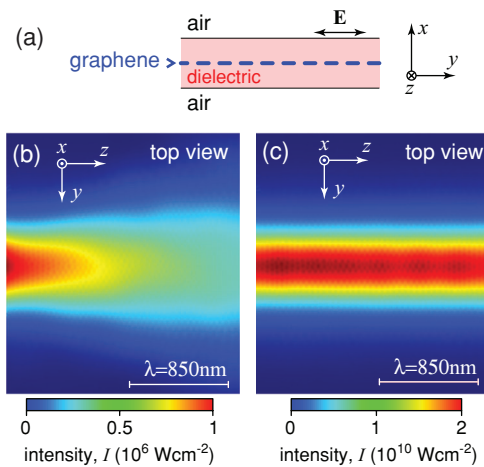


Figure 1 (online color at: www.lpr-journal.org) Geometry and TE soliton formation. Panel (a) depicts the lateral view of the considered geometry: a dielectric waveguide with a graphene monolayer located in the center. The intensity of a propagating beam evaluated at the graphene sheet is rendered in panel (b) for the low intensity regime, and in panel (c) for the soliton (high intensity) case.

vector Maxwell equations and solved self-consistently in the continuous wave regime using the finite element method [13].

For the case depicted in Fig. 1(b), the initial solution for the iterative method has a form of a TE-polarized beam propagating in the z -direction with a gaussian shape along the y -direction and a waveguide profile in the x -direction. On each step of the iterative process, the EM fields are calculated by solving the propagation problem with the eigenmode solution introduced as a source. In these calculations, we neglect third-order nonlinear effects in the high-index dielectric material surrounding the graphene layer. This assumption is justified by the fact that the magnitude of the third-order nonlinear optical susceptibility in conventional high-index dielectric media is several orders of magnitude smaller than the one characterizing graphene.

Figure 1 illustrates the formation of a non-diffracted beam at an operating wavelength $\lambda_0 = 850$ nm and for a dielectric waveguide of thickness 300 nm, characterized by a linear dielectric permittivity, $\epsilon_d = 2.25$. When the beam intensity (defined as the modulus of the Poynting vector) at maximum is low ($I < 10^9$ W/cm²), the system operates in the linear regime and the beam diffracts while traveling in this structure, see Fig. 1(b). However, our numerical calculations show that, for high enough intensity ($I > 10^9$ W/cm²), the nonlinearity of graphene can compensate diffraction leading to the formation of EM solitons. This is illustrated in Fig. 1(c), computed for $I = 10^{10}$ W/cm², showing a non-diffracted beam with a lateral size of the order of λ_0 . The soliton field is laterally confined due to the self-induced change of the effective refractive index, similarly to what happens to a beam traveling within a bulk nonlinear waveguide [10]. In contrast to a conventional nonlinear waveguide, in which the nonlinear index

change occurs in the whole volume, here in our system the 3D beam is laterally self-guided thanks to the nonlinearity that is only present in the 2D graphene sheet. We stress that these spatial solitons, sustained by a single graphene sheet, are very different to those supported by a metamaterial composed of graphene-dielectric superlattices in the terahertz regime, which propagate perpendicularly to the graphene layers [14]. We also emphasize that the class of bright self-guided solitonic modes observed in Fig. 1(c) could not be supported by a thin metal film. In general, for the frequency range considered in this work, metal films of nanometric thickness feature complex values of the nonlinear third-order susceptibility, $\chi^{(3)}$, such that $\text{Re}\chi^{(3)} < 0$ and $\text{Im}\chi^{(3)}$ is positive and large [15], i.e., they display self-defocusing nonlinearities with large nonlinear absorption losses.

Optical solitons in graphene should be observable with current samples and moderate beam intensities. Although the considered peak intensity in Fig. 1(c) is much higher than the reported damage threshold of graphene for continuous wave excitation, $I_{\text{CWth}} \sim 10^6$ W/cm² [16], it is still well below the damage threshold of graphene for 200 fs pulses, $I_{\text{Pth}} \sim 10^{12}$ W/cm² [17]. Our continuous wave description of the soliton propagation under pulsed excitation is fully justified as the optical cycle associated with $\lambda_0 = 850$ nm is two orders of magnitude shorter than a 200 fs pulsed beam.

Additional insight on the physical process can be gained from the study of the beam profile. Figure 2(a) renders the normalized transversal electric field profile $|\mathbf{E}(x, y)|$ of the calculated 3D eigenmode for $I = 1.8 \times 10^{10}$ W/cm² (high intensity regime). The field cross-section along the y -direction [see Fig. 2(b)] can be accurately fitted by the function $\text{sech}(y/w(x))$, where $w(x)$ is a measure of the lateral beam size, which slightly depends on x . This functional form for graphene EM solitons will be discussed later on. On the other hand, the confinement of the E -field along the x -direction is governed by the total internal reflection at the boundaries of the dielectric waveguide. The normalized E -field cross-section along the x -direction changes as the y coordinate is varied (see Fig. 2(c)). This change is more significant than in planar nonlinear waveguides and represents a distinct manifestation of the unusually large nonlinear optical current supported by the 2D graphene sheet that, in the present case, substantially exceeds the linear one.

We turn now to analyze the dependence of soliton width (characterized by the full width at half maximum (FWHM), a , of the soliton E -field) on the external intensity illuminating the system. In order to do this, we have computed the nonlinear eigenmodes for several peak E -field amplitudes in the graphene layer. The results, in terms of the corresponding intensity distributions (which in each case have been normalized to the maximum beam intensity), are summarized in the inset of Fig. 3. As the maximum value of the E -field in the graphene layer ($|E|_{\text{max}}$) is increased from 0.8×10^8 V/m (bottom panel) to 4.2×10^8 V/m (top panel), a decreases from $a = 2$ μm (more than 2 times the wavelength of the external illumination) to $a = 0.253$ μm (well inside the subwavelength regime). The results displayed in Fig. 3 represent a novel instance, in a strict 2D system,

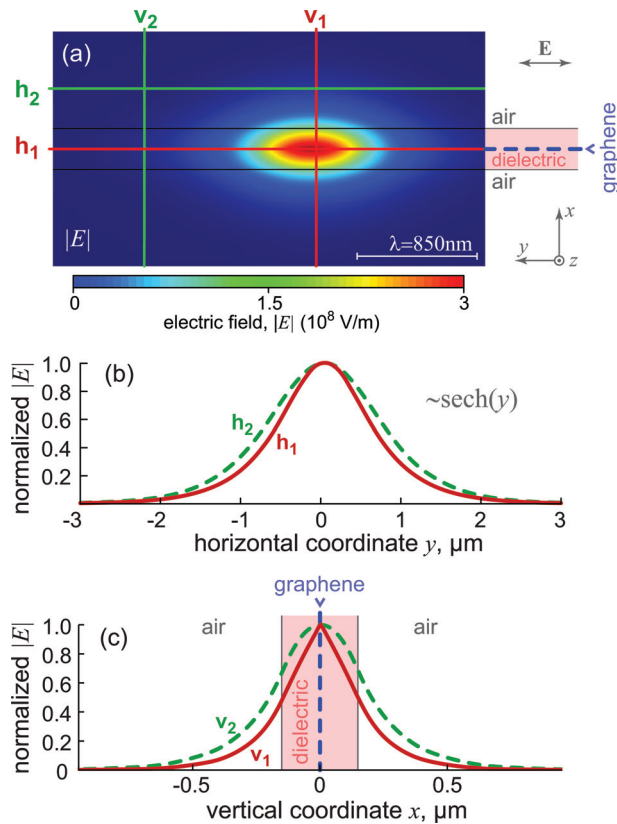


Figure 2 (online color at: www.lpr-journal.org) Soliton profile analysis. Panel (a) shows the transversal E -field distribution, $|E|$, of the soliton mode for the case in which the peak intensity is $I = 1.8 \times 10^{10} \text{ W/cm}^2$. The horizontal cross-sections h_1 and h_2 of the normalized E -field (panel b) display a conventional soliton profile proportional to $\text{sech}(y)$. For the vertical cross-sections (panel c), the E -field at v_2 has the standard profile of a linear waveguide mode. For the cross-section evaluated at v_1 , the shape of the beam corresponds to that of a nonlinear system. The filled area on the panel (c) shows the location of the dielectric waveguide.

on how the balance between nonlinearity and diffraction can yield self-guided propagating beams with subwavelength lateral confinement. In this context, it is important to point out that when graphene losses are incorporated into the calculations (these losses stem from the linear part of the graphene conductivity), the propagation length L of the soliton, defined as $L = 1/2\text{Im}(\beta_{\text{NL}})$, β_{NL} being the complex propagation constant of the nonlinear mode, is barely dependent on a . In the case considered in Fig. 3, we find that the propagation length slightly decreases with a in a monotonous manner, being $L = 20 \mu\text{m}$ for $a = 2 \mu\text{m}$ and $L = 15 \mu\text{m}$ for $a = 0.25 \mu\text{m}$. This virtual independence of the propagation length on the field confinement is very different to what is observed in other subwavelength-confined EM modes as, for example, surface plasmon polaritons.

To account for the physical origin of the above described dependence of the soliton width on the peak electric field amplitude, we have adapted to this problem the theoretical approaches used to describe soliton formation in con-

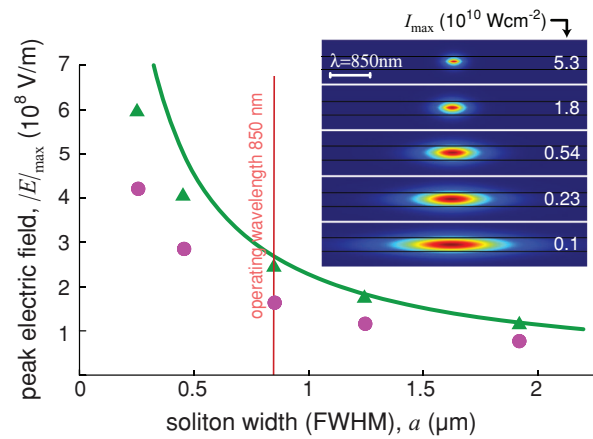


Figure 3 (online color at: www.lpr-journal.org) Dependence of the soliton width with the input intensity. Main panel presents the peak electric field dependence with the soliton width. Circular dots represent the values obtained with the full nonlinear calculation whereas the solid line renders the results from the quasi-analytical treatment (see main text). When the profile $\hat{\mathbf{A}}(x)$ and the propagation constant β corresponding to the numerical calculation is included (triangular dots), the agreement between analytics and numerics is improved. The inset shows the normalized intensity distributions for the five soliton widths considered in the main panel. The peak intensity I_{max} is indicated for each profile. The operating wavelength in all cases is $\lambda_0 = 850 \text{ nm}$.

ventional 3D nonlinear optical materials [8–10]. For this quasi-analytical treatment, we employ the 3D modeling of the graphene layer, which, as mentioned before, gives virtually the same results as a description based on a strictly 2D conductivity. Within this approach the propagation of light *inside* the graphene layer is formulated in terms of the non-homogeneous vector Helmholtz's equation,

$$c^2 \epsilon_0 \left[\left(\frac{n_s}{c} \right)^2 \frac{\partial^2}{\partial t^2} - \nabla^2 \right] \mathbf{A}(\mathbf{r}, t) = \mathbf{j}_{\text{NL}}(\mathbf{r}, t) \quad (1)$$

where $\mathbf{A}(\mathbf{r}, t)$ is the magnetic potential vector (i.e., $\mathbf{E}(\mathbf{r}, t) = -\partial \mathbf{A}(\mathbf{r}, t)/\partial t$, choosing the gauge $\nabla \cdot \mathbf{A} = 0$) and n_s is the linear refractive index of graphene. To solve Eq. ((1)), we start by assuming that its solutions are of the form

$$\mathbf{A}(\mathbf{r}, t) = \frac{1}{2} [\hat{\mathbf{A}}(x) F(z, y) \exp[i(\beta z - \omega t)] + c.c.] \quad (2)$$

where $\hat{\mathbf{A}}(x)$ is, in principle, an arbitrary function that governs the confinement of the EM field along the x -direction (see definition of axes in Fig. 1). As deduced from Eq. ((2)), $\hat{\mathbf{A}}(x)$ also defines the polarization of the considered modal profile. The EM field profile in the graphene plane is controlled by the complex function $F(z, y)$, whereas the corresponding propagation constant along the z -direction is given by β .

Now, we insert Eq. ((2)) into Eq. ((1)), we apply the slowly varying amplitude approximation, and we project

the left and right-hand-side of the resulting equation over $[\hat{\mathbf{A}}_{\parallel}(x)]^{*T}$ (where $[\]^{*T}$ stands for the transpose conjugate). Then, we define the auxiliary function $f(z, y) \equiv F(z, y) \exp(-i\phi z)$ (where $\phi \equiv (k_s^2 - \beta^2 + I_2/I_1)/2$, $k_s \equiv n_s^2 \omega^2/c^2$, $I_1 \equiv \int_{-\infty}^{\infty} dx |\hat{\mathbf{A}}_{\parallel}(x)|^2$ and $I_2 \equiv \int_{-\infty}^{\infty} dx [\hat{\mathbf{A}}_{\parallel}(x)]^{*T} \partial^2 \hat{\mathbf{A}}_{\parallel}(x) / \partial x^2$). Using these definitions, after some algebra, one finds that Eq. ((1)) can be rewritten in terms of the function $f(z, y)$ as

$$2i\beta \frac{\partial f(z, y)}{\partial z} + \frac{\partial^2 f(z, y)}{\partial y^2} + g|f(z, y)|^2 f(z, y) = 0 \quad (3)$$

where $g \equiv \frac{3}{4} \omega^4 \chi_{\text{gr}}^{(3)} I_3 / I_1 c^2$, with $I_3 \equiv \int_{-d_{\text{gr}}/2}^{+d_{\text{gr}}/2} dx |\hat{\mathbf{A}}_{\parallel}(x)|^4$. The crucial point to realize is that Eq. ((3)) corresponds to the standard form of the *nonlinear Schrodinger equation*, whose solutions have a canonical first-order soliton form [8, 10],

$$f(y, z) = \frac{1}{w} \sqrt{\frac{2}{g}} \text{sech}(y/w) \exp(iz/2\beta w^2) \quad (4)$$

where w is the conventional definition of the soliton width, which in terms of the soliton FWHM is given by $w \approx a/2.64$. Physically, Eq. ((3)) and its corresponding solution given in Eq. ((4)) can be interpreted as those governing the propagation of light in a special class of index-guided waveguide in which the refractive index contrast between the core and the cladding is induced by the intensity of the propagating beam itself. Importantly, Eq. ((4)) confirms the existence of soliton solutions in graphene, as observed in the numerical experiments reported in Figs. (1)–(3). Notice that the strength of the effective nonlinearity is characterized by the parameter g , which is proportional to both $\chi_{\text{gr}}^{(3)}$ (related to the intrinsic nonlinearity of graphene in a free-standing configuration) and I_3/I_1 , which provides a measure of the fraction of EM energy that flows inside the graphene sheet.

Inspired by the theoretical approaches used traditionally in nonlinear optics [8–10], we assume that both the vector function $\hat{\mathbf{A}}(x)$ and the propagation constant β of the modal profile correspond to those obtained numerically for the linear counterpart of the structure sketched in Fig. 1(a). The results computed within this approximation are displayed in Fig. 3 (see solid line), showing a qualitative agreement between the analytical results and the full numerical calculations. We emphasize that no fitting parameters are used in this comparison. The discrepancy between analytics and full numerics becomes larger as the value of a decreases. This fact can be ascribed to the difference between the profile $\hat{\mathbf{A}}(x)$ obtained for the linear case and that computed numerically for the full nonlinear problem, which increases as a decreases. This point is confirmed by the additional results displayed in Fig. 3 (triangular points), which show how the agreement between analytics and numerics improves when we introduce in Eq. ((2)) both the self-consistent profile, $\hat{\mathbf{A}}(x)$ (obtained at $y = 0$), and the propagation constant β corresponding to our nonlinear simulations. The remaining difference can be traced back to the separability in the x

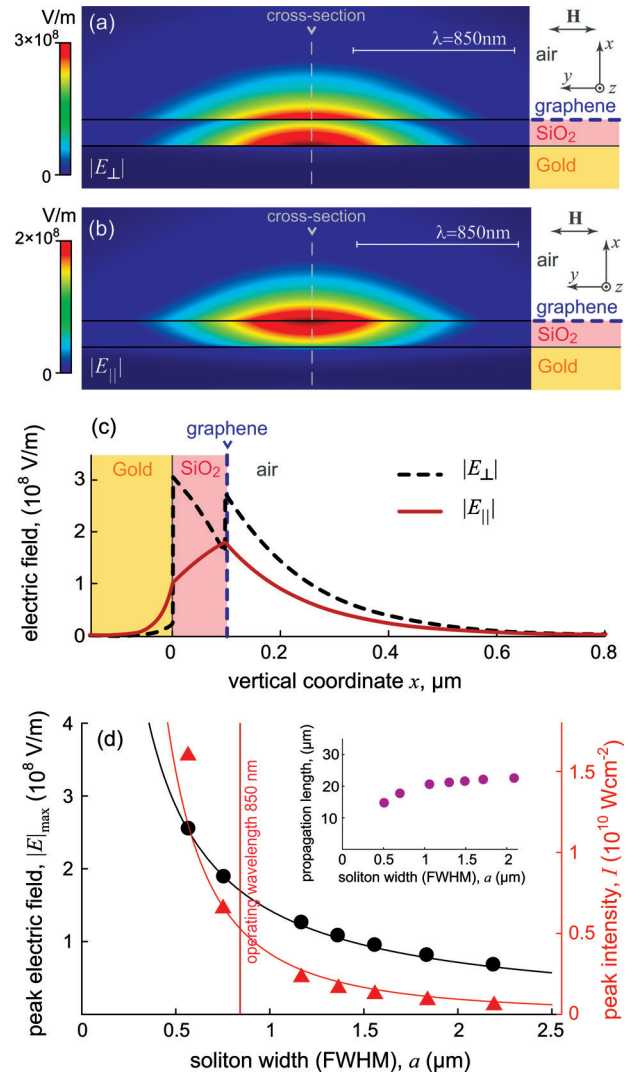


Figure 4 (online color at: www.lpr-journal.org) TM soliton formation. The geometry consists of the graphene monolayer and gold half-space, separated by a silicon dioxide layer of thickness of 100 nm. The operating wavelength is $\lambda_0 = 850$ nm. The density plots in panel (a) and (b) render the transversal $|E_{\perp}|$ and in-plane $|E_{\parallel}|$ components of the electric field, respectively, associated with the excitation of a TM SPP-soliton. Panel (c) renders the transversal $|E_{\perp}|$ (solid lines) and in-plane $|E_{\parallel}|$ (dashed curves) along the vertical direction depicted in the upper panels. Panel (d) shows the dependence on soliton FWHM, a , of the peak E -field amplitude (dots) and the peak intensity I (triangles), evaluated at the graphene monolayer. The solid lines are fittings to a $1/a$ and $1/a^2$ functions for peak E -field and intensity, respectively. Inset to panel (d) renders the calculated propagation length dependence on a .

and (y, z) coordinates implied by Eq. ((2)) that cannot fully account for the complexity of the graphene EM solitons.

Finally, we show that TM-polarized optical solitons can also propagate along a graphene monolayer. A graphene structure that is able to support these TM optical solitons is rendered on Fig. 4. Here the vertical confinement is provided by a surface plasmon polariton (SPP) mode that is

propagating on the interface between gold and a dielectric film. The graphene monolayer, which is characterized by a large nonlinear third-order susceptibility, must be separated from the metal surface by a dielectric spacer. We have chosen a 100 nm silicon dioxide layer, just for proof-of-principles purposes. Our calculations show that this system supports the propagation of a very peculiar class of TM soliton, which results from the *hybridization* between the SPP supported by the metal-dielectric interface and the soliton propagating in the graphene sheet. The computed distributions of the transversal $|E_{\perp}|$ and in-plane $|E_{\parallel}|$ components of the electric field of this hybrid SPP-soliton solution is plotted in Fig. 4(a,b) and displays exactly the conventional solitonic profile $\sim \text{sech}(y)$ along the y -direction. The in-plane $|E_{\parallel}|$ component of the electric field of hybrid SPP-soliton is responsible for nonlinear effect and provides diffraction compensation. This component reaches its maximum value at the graphene layer, see Figs. 4(b) and 4(c).

The dependence of the soliton width with the peak E -field amplitude rendered in Fig. 4(d) is very similar to that found for TE optical solitons, predicting the existence of subwavelength optical solitons also for this polarization. Similarly to the case of the TE geometry, the propagation length of the hybrid SPP-soliton is weakly dependent on the soliton width, the points on the inset of Fig. 4(d). In contrast to the TE case, in the case of hybrid SPP-soliton the propagation length is almost independent on soliton width when this is larger than the wavelength (reflecting that, in this case, losses occur mainly in the metal). For smaller soliton widths the propagation length decreases with a , and our calculations show that the losses occur mainly in the graphene layer.

To analyze the effect of losses on the beam shape we calculated how the beam width changes as the soliton propagates. In the lossless case, the soliton width remains constant while propagating. When realistic losses in both metal and graphene were considered, the soliton beam broadens with distance. As a representative example, when the incident beam width is 0.7 μm , the computed soliton broadening is 30% after traveling a distance of 4 μm . In comparison, in the linear regime the corresponding value is 150%. This behavior is similar to that found for SPP-solitons appearing at the interface between a metal and a semi-infinite Kerr dielectric [18]. Notice that considering a dielectric with a higher dielectric constant would allow increasing the confinement in the direction normal to the surface. However, this would push the field towards the metal, with a corresponding increase in losses and a decrease in the propagation length of the soliton.

In conclusion, we have demonstrated that graphene monolayers can support both TE and TM spatial optical solitons due to the extremely large magnitude of its nonlinear third-order susceptibility. Moreover, we have shown that for feasible values of the input intensity these quasi-one dimensional optical solitons can have a subwavelength lateral width. We have also developed a quasi-analytical model that has a semi-quantitative value and that is able

to predict the field intensities needed for soliton formation. The existence of subwavelength optical solitons adds a new capability to the already broad range of optical phenomena associated with graphene structures.

Acknowledgements. This work has been partially funded by the Spanish Ministry of Science and Innovation under contracts MAT2011-28581-C02 and CSD2007-046-NanoLight.es and grants RyC-2009-05489 and JCI-2008-3123. Financial support by the European Research Council (contract 290981) is also acknowledged.

Received: 18 September 2012, **Revised:** 5 November 2012,
Accepted: 13 November 2012

Published online: 31 December 2012

Key words: Graphene, solitons, nonlinear optics.

References

- [1] K. S. Novoselov, A. K. Geim, S. V. Morozov, D. Jiang, Y. Zhang, S. V. Dubonos, I. V. Grigorieva, and A. A. Firsov, *Science* **306**, 666 (2004).
- [2] A. H. Castro Neto, F. Guinea, N. M. R. Peres, K. S. Novoselov, and A. K. Geim, *Rev. Mod. Phys.* **81**, 109 (2009).
- [3] F. Bonaccorso, Z. Sun, T. Hasan, and A. C. Ferrari, *Nature Photon.* **4**, 611 (2010).
- [4] M. Liu, X. Yin, E. Ulin-Avila, B. Geng, T. Zentgraf, L. Ju, F. Wang, and X. Zhang, *Nature* **474**, 64 (2011).
- [5] S. A. Mikhailov, *Europhys. Lett.* **79**, 27002 (2007).
- [6] K. L. Ishikawa, *Phys. Rev. B* **82**, 201402 (2010).
- [7] E. Hendry, P. Hale, J. Moger, A. Savchenko, and S. Mikhailov, *Phys. Rev. Lett.* **105**, 097401 (2010).
- [8] R. W. Boyd, *Nonlinear Optics* (Academic Press, New York, 1992).
- [9] G. P. Agrawal, *Nonlinear Fiber Optics*. (Academic Press, San Diego, 2001).
- [10] Y. Kivshar and G. Agrawal, *Optical Solitons* (Academic Press, New York, 2003).
- [11] Y. V. Kartashov, B. A. Malomed, and L. Torner, *Rev. Mod. Phys.* **83**, 247 (2011).
- [12] Y. Liu, G. Bartal, D. Genov, and X. Zhang, *Phys. Rev. Lett.* **99**, 153901 (2007).
- [13] We have used the implementation of the finite element method provided by the commercial software COMSOL Multiphysics.
- [14] H. Dong, C. Conti, and F. Biancalana, arXiv:1107.5803v1 (2011).
- [15] E. Xenogiannopoulou, P. Aloukos, S. Couris, E. Kaminska, A. Piotrowska, and E. Dynowska, *Opt. Comm.* **275**, 217 (2007).
- [16] B. Krauss, T. Lohmann, D. H. Chae, M. Haluska, K. von Klitzing, and J. H. Smet, *Phys. Rev. B* **79**, 165428 (2009).
- [17] A. Roberts, D. Cormode, C. Reynolds, T. Newhouse-Illige, B. J. LeRoy, and A. S. Sandhu, *Appl. Phys. Lett.* **99**, 051912 (2011).
- [18] A. R. Davoyan, I. V. Shadrivov, and Y. S. Kivshar, *Opt. Express* **17**, 21732 (2009).